Russian Physics Journal, Vol. 51, No. 9, 2008

ELECTRONIC STRUCTURE OF GRAIN BOUNDARIES IN THE $Fe_{86} - Mn_{12.7} - C_{1.3}$ ALLOY

A. V. Nyavro,[1] V. N. Cherepanov,[1] V. G. Arkhipkin,[3] L. I. Kveglis,[4] and V. A. Musikhin[2]

UDC 669.245: 538.915

The importance of studying Fe–Mn–C *alloys is related to their wide use as constructional materials in mechanical engineering. In this work an effort has been made to elucidate the physical origin of the magnetization in austenitic steels by calculating the electronic structure of grain boundaries. To theoretically investigate the magnetic properties of a crystal of ferromagnetic bcc iron, the wave functions of the iron atom calculated in view of the spin polarization of a core by the Hartree–Fock method with local exchange-correlation potentials have been used as base functions. This has made it possible to optimize the choice of a zero approximation for the description of the electronic states of ferromagnetic iron and to attain good agreement with the experimental values of the magnetic moment ($\mu_{theor} = 2.23\mu_B$, $\mu_{exp} = 2.218\mu_B$), of the exchange splitting of the crystal term P_4 ($\Delta_{theor} = \Delta_{exp} = 0.112$ Ry), and of the cross-sections of the Fermi surface. A similar approach has been used to investigate the magnetic states of clusters (nanoclusters) based on the method of scattered waves. The approach developed for clusters of the alloy under investigation makes it possible to calculate the alloy magnetic properties in relation to the cluster size for a varied lattice parameter.*

INTRODUCTION

Calculations of the magnetic properties of a bcc iron crystal performed by different authors show that the electronic characteristics strongly depend both on the calculation method and on the choice of the initial approximation used to calculate the energy bands for different spin subsystems. Therefore, the problem of choosing the best approximation for the electron density and, accordingly, for the electronic potential in a theoretical study of the electronic spectrum and physical properties of magnetic crystals is of critical importance: the choice of the zero approximation can be decisive for the convergence of the self-coordinated procedure. We have calculated the parameters of a Fe atom in a spin-restricted (RHF) and spin-unrestricted (UHF) approximations of the Hartree–Fock method by setting different configurations of valence electrons. This allowed us to simulate the distribution of the electron density of an atom placed in a crystal. Based on the atomic data, the crystal potential and electronic spectrum were calculated. The band spectrum was calculated by the Green function method. Investigations of the spectrum of a crystal, and of the density of states and calculations of the magnetic moment and other physical characteristics allow one to optimize the choice of a zero approximation, namely, to find the electron configuration of an atom that enables a correct description of various physical properties of the crystal.

1. UHF WITH LOCAL EXCHANGE-CORRELATION POTENTIALS FOR ATOMS

The system of Hartree–Fock equations with a local exchange-correlation potential (Hartree–Fock–Slater equations) in the UHF approximation can be written as

[1]Tomsk State University, Tomsk, Russia, e-mail: vnch@phys.rsu.ru; [2]Siberian Federal University, Krasnoyarsk, Russia; [3]L. V. Kirenskii Physics Institute of the Siberian Branch of the Russian Academy of Sciences, Krasnoyarsk, Russia; [4]East-Kazakhstan Technical University, Ust Kamenogorsk, Kazakhstan. Translated from Izvestiya Vysshikh Uchebnykh Zavedenii, Fizika, No. 9, pp. 83–88, September, 2008. Original article submitted June 04, 2008.

$$\left[-\frac{d^2}{dr^2}+\frac{l(l+1)}{r^2}-\frac{2Z}{r}+V_{\mathrm{C}}(r)-V_X^{\sigma}(r)\right]P_{nl\sigma}(r)=\varepsilon_{nl\sigma}P_{nl\sigma}(r)\,. \tag{1}$$

The number of equations in system (1) is equal to the number of subshells in the atom under consideration, that is, to the number of sets of quantum states with numbers $\{nl\sigma\}$ taken into account. In the system of equations (1), Z is the charge of the nucleus; $P_{nl\sigma}(r)$ are the radial wave functions that describe the states of electrons in the subshell with quantum numbers $\{nl\sigma\}$, where σ specifies the spin projection on the z-axis; $V_{\mathrm{C}}(r)$ is the electron Coulomb interaction potential

$$V_{\mathrm{C}}(r)=2\left[\frac{1}{r}\int_0^r dr'\rho(r')+\int_r^{\infty}\frac{dr'}{r'}\rho(r')\right], \tag{2}$$

and $V_X^{\sigma}(r)$ is the exchange-correlation potential. In terms of the X_α method it can be represented in the form

$$V_{X\alpha}^{\sigma}=6\alpha\left(\frac{3}{8\pi}\rho^{\sigma}(\bar{r})\right)^{1/3}. \tag{3}$$

In formulas (1) – (3), $\rho(r)$ and $\rho^{\sigma}(r)$ are the total and the spin electron density, which can be written as

$$\rho(r)=\frac{1}{4\pi}\sum_{nl\sigma}q_{nl\sigma}\left|R_{nl\sigma}(r)\right|^2; \tag{4}$$

$$\rho^{\sigma}(r)=\frac{1}{4\pi}\sum_{nl}q_{nl\sigma}\left|R_{nl\sigma}(r)\right|^2, \tag{5}$$

where $q_{nl\sigma}$ are the occupation numbers of subshells with different spin projections; $R_{nl\sigma}(r) = P_{nl\sigma}(r)/r$, and $\rho(r)=\sum_{\sigma}\rho^{\sigma}(r)=\rho^{\uparrow}(r)+\rho^{\downarrow}(r)$.

To solve the system of equations (1) as applied to multielectron atoms, it is necessary to use numerical methods. We have developed a code for numerically solving the system of equations (1). The solution is sought by the self-coordination method. Calculations can be performed for any atom of the Periodic System both in the spin-restricted (RHF) and in the UHF approximation.

Table 1 lists the results of calculations for a Fe atom with an optimized exchange potential $V_{X\alpha}^{\sigma}$ for $\alpha = 0.71151$ [1]. The use of the electron density obtained for the $(1s)^2(2s)^2(2p)^6(3s)^2(3p)^6(3d)^6(4s)^2$ configuration of the ground state of a Fe atom in the RHF approximation in the investigation of a ferromagnetic crystal of iron gives no way of obtaining simultaneously good data on the band spectrum, density of states, and magnetic moment. The account of the spin polarization of a Fe atom in the UHF approximation for the configuration

$$(\varphi_{1s\alpha})^1(\varphi_{1s\beta})^1(\varphi_{2s\alpha})^1(\varphi_{2s\beta})^1\cdots(\varphi_{3p\alpha})^3(\varphi_{3p\beta})^3(\varphi_{3d\alpha})^5(\varphi 3d_{\beta})^1(\varphi_{4s\alpha})^1(\varphi_{4s\beta})^1,$$

where α and β are the spin projections on the z-axis, also does not yield reasonable results. The reason is that the overlap of the electron shells of atoms in a crystal results in a partial delocalization of the 3d electrons in a Fe atom and in hybridization of the 4s and 3d electrons, and the magnetic moment in the crystal decreases compared to $\mu = 4\mu_B$ of a free atom. The decrease in magnetic moment must be taken into account when choosing an electron configuration suitable to describe an atom in a crystal. We have considered the exited configurations of a Fe atom in the UHF approximation with fractional occupation numbers

TABLE 1. The Energy Levels ($-\varepsilon_i$) and the Total Energy ($-E^t$) of a Fe Atom Calculated in the RHF and UHF Approximations with the Local Exchange Potential $V_{X\alpha}^{\sigma}$ ($\alpha = 0.71151$) for Various Configurations of Valence Electrons (Ry).

State	RHF	UHF			
	$(3d)^6(4s)^2$	$(3d_\alpha)^5\,(3d_\beta)^1$ $(4s_\alpha)^1\,(4s_\beta)^1$	$(3d_\alpha)^{4.08}\,(3d_\beta)^{1.92}$ $(4s_\alpha)^{1.02}\,(4s_\beta)^{0.98}$	$(3d_\alpha)^{4.09}\,(3d_\beta)^{1.91}$ $(4s_\alpha)^{1.01}\,(4s_\beta)^{0.99}$	$(3d_\alpha)^{4.1}\,(3d_\beta)^{1.9}$ $(4s_\alpha)^1\,(4s_\beta)^1$
$\varepsilon_{1s\alpha}$		509.2274	509.2649	509.2678	509.2677
$\varepsilon_{1s\beta}$	509.2808	509.2260	509.2640	509.2669	509.2689
$\Delta\varepsilon_{1s}$		0.0009	0.0009	0.0009	0.0008
$\varepsilon_{2s\alpha}$		59.2922	59.2926	59.2937	59.2922
$\varepsilon_{2s\beta}$	59.2594	59.1147	59.1958	59.1959	59.1936
$\Delta\varepsilon_{2s}$		0.1775	0.0968	0.0978	0.0987
$\varepsilon_{2p\alpha}$		51.2626	51.2723	51.2736	51.2718
$\varepsilon_{2p\beta}$	51.2504	51.1280	51.1988	5.1993	51.1969
$\Delta\varepsilon_{2p}$		0.1346	0.0715	0.0743	0.0749
$\varepsilon_{3s\alpha}$		6.8353	6.7830	6.7839	6.7838
$\varepsilon_{3p\beta}$	6.8944	6.4599	6.5798	6.5788	6.5769
$\Delta\varepsilon_{3d}$		0.3754	0.2032	0.2051	0.2069
$\varepsilon_{3p\alpha}$		4.4838	4.4318	4.4325	4.4342
$\varepsilon_{3p\beta}$	4.3447	4.1159	4.2325	4.2316	4.2296
$\Delta\varepsilon_{3p}$		0.3677	0.1993	0.2009	0.2044
$\varepsilon_{3d\alpha}$		0.6734	0.6245	0.6251	0.3299
$\varepsilon_{3d\beta}$	0.5452	0.3448	0.4458	0.4452	0.4437
$\Delta\varepsilon_{3d}$		0.3286	0.1787	0.1799	0.1812
$\varepsilon_{4s\alpha}$		0.3803	0.3656	0.3650	0.3263
$\varepsilon_{4s\beta}$	0.3448	0.3044	0.3225	0.3233	0.3240
$\Delta\varepsilon_{4s}$		0.0759	0.0431	0.0417	0.0403
E^t	2488.4899	2488.6430	2488.5824	2488.6052	2488.5368

$$(\varphi_{1s\alpha})^1(\varphi_{1s\beta})^1(\varphi_{2s\alpha})^1(\varphi_{2s\beta})^1\cdots(\varphi_{3p\alpha})^3(\varphi_{3p\beta})^3(\varphi_{3d\alpha})^x(\varphi 3d_\beta)^y(\varphi_{4s\alpha})^u(\varphi_{4s\beta})^v, \quad (6)$$

where x, y, u, and v are the occupation numbers of the valence 3d and 4s shells. The electron density obtained for the atomic configuration

$$(\varphi_{1s\alpha})^1(\varphi_{1s\beta})^1(\varphi_{2s\alpha})^1(\varphi_{2s\beta})^1\cdots(\varphi_{3p\alpha})^3(\varphi_{3p\beta})^3(\varphi_{3d\alpha})^{4,1}(\varphi 3d_\beta)^{1,9}(\varphi_{4s\alpha})^1(\varphi_{4s\beta})^1 \quad (7)$$

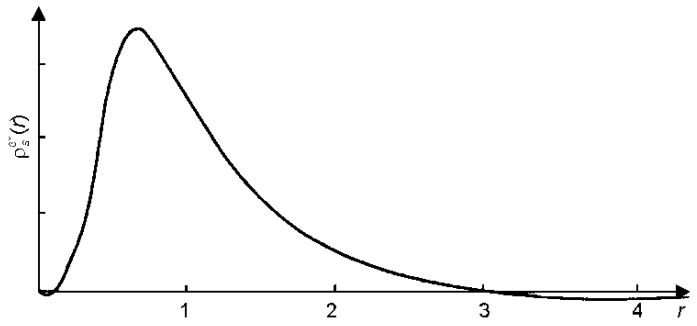

Fig. 1. Spin atomic electron density $\rho_s^{at}(r)$ for the configuration (7).

and used for the calculation of the electronic spectrum of a crystal [2], provides an agreement both with predictions of other authors [3–10] and with experiment [11].

2. CALCULATIONS OF THE CRYSTAL POTENTIAL AND SPECTRUM FOR BCC IRON

For the calculation of the band spectrum of a crystal in the zero approximation, the crystal electron density was taken in the form of a superposition of atomic densities. The contributions of the atomic densities of nine coordination spheres were considered:

$$\rho^{cr}(r) = \sum_p \frac{n_p}{2rR_p} \int_{R_p - r}^{R_p + r} \rho^{at}(r')r'dr' , \tag{8}$$

where R_p is the radius of the pth coordination sphere and n_p is the number of atoms in the sphere. The electron density of the atom, $\rho^{at}(r)$, is calculated from the wave functions, obtained on solving the system of equations (1), by formulas (4)–(5) for the configuration (7). The spin atomic density

$$\rho_s^{at}(r) = \left(\rho^{\uparrow}(r) - \rho^{\downarrow}(r)\right)r^2 \tag{9}$$

is presented in Fig. 1. Note that the spin density $\rho_s^{at}(r)$ is represented by an alternating-sign curve: Near the nucleus $\rho_s^{at}(r)$ is positive, then, with increasing r, it becomes negative, in the region of the maximum localization of 3d electrons ($r \sim 1$ a. u.) it is positive, and at large r it again becomes negative because of the polarization of the s–p-shells of the atom by the 3d electrons. The atomic density $\rho_s^{at}(r)$ and the crystal density $\rho_s^{cr}(r)$ differ inappreciably.

For the crystal potential, the *muffin-tin* approximation was used. The Coulomb part of the potential is formed by two contributions made by the charge of the nucleus and by the potential of the electrostatic interaction of electrons, which was calculated by solving the Poisson equation inside the Slater sphere. For the exchange-correlation potential, the Gunnarson–Lundqvist approximation [12] was used in the calculations of the electronic spectrum of the crystal.

The electron energy distribution was determined from the solution of the secular equation of the Green function method written for each spin subsystem. Table 2 presents the results of the calculation of the exchange splitting of electron energy terms in bcc iron. It can be seen that the exchange splitting obtained in band calculations is different in value for the s- and d-states. Moreover, the exchange splitting depends on the wave vector $\boldsymbol{k}$. Thus, we have $\Gamma_1\uparrow - \Gamma_1\downarrow = 0.032$ Ry for the level Γ_1 (s-type symmetry) and 0.159, 0.149, and 0.189 Ry for the d-symmetry levels Γ_{12}, Γ'_{25}, and H'_{25}, respectively.

From Table 2 it also follows that the exchange splitting values obtained by us well agree with predictions of other authors [3–10]. Good agreement has also been attained between our prediction and the experimental value for the splitting of the crystal term P_4 [11].

TABLE 2. Exchange Splitting of the Electron Energy Terms in a Crystal (Ry). The Lattice Constant Value Used in Our Calculations Was 5.4 a. u.

Term	Our calculations	[3]	[4]	[5]	[6]	[7]	[8]	[9][a]	[10][b]	[11]
Γ'_{25}	0.149			0.134	0.141	0.149		0.168	0.185	
H_{12}	0.108	0.088	0.095	0.111	0.121	0.107				
N_2	0.135			0.121	0.128	0.134				
Γ_1	0.032	0.039	0.034	0.012	0.030	0.029	0.015			
P_4	0.112			0.098			0.096	0.122	0.139	0.112
P_3	0.164						0.172			

Note: Here, in Table 3, and in Table 4 the superscripts “a” and “b” refer to the nonrelativistic calculations [9] and to the semirelativistic calculations [9], respectively.

TABLE 3. Electron Energy Band Width for Ferromagnetic bcc Iron

Term	Our calculations	[3]	[5]	[6]	[7]	[8]	[9][a]	[9][b]	[11]
$(\Gamma_{12}-\Gamma'_{25})^{\uparrow}$	0.106		0.102	0.097	0.111		0.108	0.102	
$(\Gamma_{12}-\Gamma'_{25})^{\downarrow}$	0.116		0.128	0.130	0.119		0.119	0.113	
$(\Gamma'_{25}-\Gamma_1)^{\uparrow}$	0.496		0.438	0.454	0.450				
$(\Gamma'_{25}-\Gamma_1)^{\downarrow}$	0.605		0.560	0.565	0.572				
$(H'_{25}-H_{12})^{\uparrow}$	0.375	0.356	0.339				0.362	0.350	
$(H'_{25}-H_{12})^{\downarrow}$	0.435	0.408	0.383				0.453	0.424	
$(P_3-P_4)^{\uparrow}$	0.207		0.194			0.182	0.217	0.190	0.228
$(P_3-P_4)^{\downarrow}$	0.260		0.254			0.258	0.280	0.254	

Comparison of the data presented in Table 1 and Table 2 shows that there is a correspondence between the splitting of *s*-, *p*-, and *d*-type atomic levels and the splitting of the relevant crystal terms. This allows the conclusion that the exchange splitting of levels in a crystal is determined by the spin polarization of the electrons localized in an atom.

The energy band widths obtained by different authors are given in Table 3. It can be seen that the greatest difference between our predictions and the data obtained by other authors is in the relative position of the *s*- and *p*–d-bands. This can be explained by using different local approximations for the exchange potential. Electrons with various values of the orbital moment differently react to a variation of the exchange potential, and, as a result, the relative position of the *s*- and *d*-bands varies.

As a whole, the results obtained show that the atomic configuration of the form (7) allows a reasonably adequate description of the electron density distribution for an atom in a crystal, resulting in a good agreement of the electronic spectrum with predictions of other authors and with experiment. Thus, the atomic base used can serve as a good zero approximation for investigating other physical characteristics of a ferromagnetic crystal.

TABLE 4. Some Electron Characteristics of Ferromagnetic Iron

Parameters	Our calculations	[5]	[8]	[9][a]	[9][b]	[10, 11]
$N(E_F)^{\uparrow}$	18.906	11.29	11.036	21.30	21.60	
$N(E_F)^{\downarrow}$	2.818	3.35	3.341	5.57	6.36	
$N(E_F)$	21.724	14.64	14.377	26.87	30.16	19.04, 27.37
μ	2.23	2.16	2.153	2.226	2.444	1.72
Δ_c	0.138	0.16	0.172			

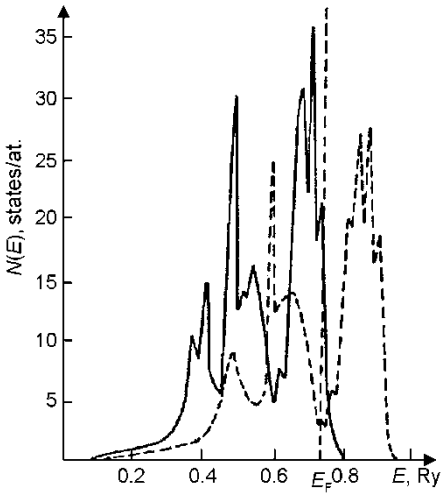

Fig. 2. Density of states for bcc iron in the spin subband of the majority of electrons (solid lines) and in that of the minority of electrons (dashed lines).

3. DENSITY OF STATES IN FERROMAGNETIC BCC IRON

From Fig. 2, which presents the curves of the density of states for two spin subbands calculated by us [2], it can be seen that these curves are similar in structure. The calculated value of the Fermi level is 0.733 Ry and the magnetic moment per atom is 2.23 μ_B. The experimental value of μ is 2.218 μ_B [1]. The spin splitting, calculated as the distance between two principal peaks of the density of states for different spin subbands, is 0.138 Ry.

Table 4 lists values of the density of states at the Fermi level for the both spin subbands and values of the magnetic moment and of the spin splitting obtained by different authors.

From the results presented it can be seen that the densities of states at the Fermi level in the spin subband of the majority of electrons are always greater than those in the spin subband of the minority of electrons. The total value of the density of states at the Fermi level is in reasonable agreement with the experimental value of this quantity.

The approach used, allowing one to choose an optimum configuration of atomic electrons in a crystal, has been demonstrated to be efficient in describing the magnetic properties of a crystal of bcc iron. This approach can also be employed to investigate the properties of compounds of complicated composition, including the transitional elements of the iron group, and in studies based on cluster models.

4. ELECTRON STRUCTURE OF GRAIN BOUNDARIES IN HADFIELD STEEL

Hadfield steel (110G13L) is widely known as a material which self-hardens under shock loading. The physicochemical mechanism of this type of self-hardening still remains obscure. A mechanical shock can give rise to mechanochemical reactions both in a bulky and in a film specimen of the Fe–Mn system. The reaction products can be both strain-induced martensite and phases having Frank–Kasper structures. The increase of the lattice parameter of austenite to 3.62 Å and the anomalous decrease of the lattice parameter of strain-hardened martensite confirm the hypothesis that Frank–Kasper clusters nucleate during shock loading. It is of interest to elucidate the reasons for the magnetization of the intergranular layer in type 110G13L ($Fe_{86}Mn_{12.8}C_{1.2}$) austenitic steels for which an anomalous increase in volume has been revealed.

The first stage of this work is a study of the electronic structure of a Fe_{87}–Mn_{13} cluster by using a cluster model. To elucidate the nature of the magnetism in the Fe_{87}–Mn_{13} alloy, having the Frank–Kasper structure FK12+FK14 (β-$Fe_{87}-Mn_{13}$), the method of scattered waves [1], which allows one to construct a local electronic structure of an alloy in view of spin polarization, was used [13]. The spectra of the density of electronic states calculated for the β-$Fe_{87}-Mn_{13}$ alloy that contains two types of clusters: Fe11Mn2, consisting of 11 Fe atoms and 2 Mn atoms (twelve-vertex structure FK12), and Fe13Mn2, consisting of 13 Fe atoms and 2 Mn atoms (fourteen-vertex structure FK14) [13], have shown that the distinction in structure of the clusters, and, as a consequence, in potentials of their atoms and wave functions, yields different magnetic moments in local fields of the β-phase. Thus, spin-polarized calculations give $<\mu> = 1.4\ \mu_B$/at. for Fe11Mn2 and $<\mu> = 0.5\ \mu_B$/at. for Fe13Mn2. The considerably lower moment obtained for the Fe13Mn2 structure can be related to the antiferromagnetic alignment of some atoms in this structure. However, the computational method [13] should be further developed for gaining more detailed knowledge on the processes that occur in the intergranular layer of austenitic steels under various actions. We anticipate that the approach based on the optimization of the atomic base of clusters proposed in this paper will make it possible to solve this problem.

REFERENCES

1. J. C. Slater, Quantum Theory of Molecules and Solids, Vol. 4: The Self-Consistent Field for Molecules and Solids, McGraw-Hill, New York (1974).
2. A. V. Nyavro, Theoretical Investigation of the Electronic States of Atoms and Atomic Condensates by the Hartree–Fock Method with Local Exchange-Correlation Potentials [in Russian], Thesis for Candidate's Degree in Phys. and Math., TSU, Tomsk (2007).
3. L. I. Vinokurova, A. T. Gapotchenko, E. S. Nukevich , *et al*., Zh. Eksper. Teor. Fiz., **76**, 1644–1654 (1979).
4. S. Wakoh and J. Jamashita, J. Phys. Soc. Jap., **21**, 1712–1729 (1966).
5. J. Callaway and G. S. Wang, Phys. Rev., **B16**, 2095–2105 (1977).
6. K. B. Harthaway, H. I. F. Jansen, and A. J. Freeman, *Ibid*., **B31**, 7603–7611 (1985).
7. V. L. Moruzzi, J. F. Janack, and A. R. Williams, Calculated Electronic Properties of Metals, Pergamon Press, New York (1978).
8. D. Bagayoko and J. Callaway, Phys. Rev., **B28**, 5419–5422 (1983).
9. W. B. Johnson, J. R. Anderson, and D. A. Papaconstantopoulos, *Ibid*., **B29**, 5327–5348 (1984).
10. H. S. Greenside and M. A. Schluter, *Ibid*., **B27**, 3111–3114 (1983).
11. D. Eastman, F. J. Himpsel, and J. A. Knapp, Phys. Rev. Lett., **44**, No. 2, 95–98 (1980).
12. O. Gunnarson and B. I. Lundqvist, Phys. Rev. B, **13**, 4274–4298 (1976).
13. V. S. Demidenko, N. L. Zaitsev, I. A. Nechaev, *et al*., Fiz. Met. Metalloved., **101**, No. 3, 1–6 (2006).